

Article

On the number of galaxies at high redshift**Lorenzo Zaninetti** ¹,¹ Dipartimento di Fisica, via P.Giuria 1,
I-10125 Turin, Italy*Received: xx / Accepted: xx / Published: xx*

Abstract: The number of galaxies at a given flux as a function of the redshift, z , is derived when the z -distance relation is non-standard. In order to compare different models, the same formalism is also applied to the standard cosmology. The observed luminosity function for galaxies of the zCOSMOS catalog at different redshifts is modelled by a new luminosity function for galaxies, which is derived by the truncated beta probability density function. Three astronomical tests, which are the photometric maximum as a function of the redshift for a fixed flux, the mean value of the redshift for a fixed flux, and the luminosity function for galaxies as a function of the redshift, compare the theoretical values of the standard and non-standard model with the observed value. The tests are performed on the FORS Deep Field (FDF) catalog up to redshift $z = 1.5$ and on the zCOSMOS catalog extending beyond $z = 4$. These three tests show minimal differences between the standard and the non-standard models.

Keywords: Cosmology; Observational cosmology; Distances, redshifts, radial velocities, spatial distribution of galaxies; Magnitudes and colors, luminosities

PACS classifications: 98.80.-k ; 98.80.Es 98.62.Py ; 98.62.Qz

1. Introduction

The linear correlation between the expansion velocity, v , and d_l , the distance in Mpc, is

$$v = H_0 d_l = c z \quad , \quad (1)$$

where H_0 is the Hubble constant $H_0 = 100h \text{ km s}^{-1} \text{ Mpc}^{-1}$, with $h = 1$ when h is not specified, c is the velocity of light, $c = 299792.458 \frac{\text{km}}{\text{s}}$ see Mohr *et al.* [1], and z is the redshift defined as

$$z = \frac{\lambda_{obs} - \lambda_{em}}{\lambda_{em}} \quad , \quad (2)$$

with λ_{obs} and λ_{em} denoting respectively the wavelengths of the observed and emitted lines as determined from the lab source, the so called Doppler effect. This linear relation can be derived from first principles, namely general relativity (GR), and is only a low- z limit of a more general relation in standard cosmology. The presence of a velocity in the previous equation has pointed the standard cosmology towards an expanding universe. The previous equation also contains a linear relation between distance and redshift, and this has pointed the experts in plasma physics towards an explanation of the redshift in terms of the interaction of light with the electrons of the intergalactic medium (IGM). In terms of plasma physics, the expansion velocity of the universe becomes a pseudo-velocity because the Universe is supposed to be Euclidean and static. The conjecture here adopted is now outlined: the redshift should be considered as a spectroscopic measure independent of the adopted cosmology. An example of this conjecture can be found at the home page of the Supernova Cosmology Project (SCP) ‘All the analyses were developed with cosmology hidden.’ The main physical explanations for the redshift are: a Doppler shift, which means an expanding universe, a general relativistic effect, see [2], a plasma effect, see [3], and a tired light effect as suggested by [4,5]. More details on the various theories which explain the cosmological redshift can be found in [6]. *A point of discussion:* The presence of physical effects which explain the redshift allows speaking of a Euclidean universe in which the distances are evaluated with the Pythagorean theorem. In a Euclidean universe, the main parameters are H_0 , z , and the distance, d , but the velocity of expansion is virtual rather than real. The aim of having a Euclidean universe is the explanation of the astronomical variables such as the redshift and the absolute magnitude and count of galaxies without GR.

Concerning the value of H_0 and Ω_M , we will adopt recent values as obtained by a mixed model which uses the cosmic microwave background (CMB) measurements at high redshift and the baryon acoustic oscillation (BAO), see [7],

$$H_0 = (69.6 \pm 0.7) \text{ km s}^{-1} \text{ Mpc}^{-1} \quad , \quad (3)$$

$$\Omega_M = 0.286 \pm 0.008 \quad . \quad (4)$$

Hubble’s constant is explained in the dynamical relativistic models beginning with [8,9]. Recently, research in the framework of modern theories on an accelerating universe has been focussed on measuring cosmological parameters such as Ω_M and Ω_Λ , see [10,11]. In the last years, the enormous progress in astronomical observations has increased the available data for galaxies up to $z = 3.36$, see the FORS Deep Field (FDF) catalog, which is made up of 300 galaxies with known spectroscopic redshift, see [12,13]. Another high redshift catalog is zCOSMOS, which is made up of 9697 galaxies up to $z = 4$, see [14]. These data demand a new formalism for the number of galaxies as a function of the redshift. At the same time, Hubble’s law can be inserted into a more precise physical framework. In order to cover these questions, Section 2 reviews some old and new derivations of Hubble’s law as well the magnitude system, and Section 3 derives a new relation for the number of galaxies as a function of the redshift.

Section 5 introduces a relativistic model for the number of galaxies as a function of the redshift and Section 6 deals with the luminosity function for galaxies at different redshifts.

2. Basic Formulae

The change of frequency of light in a gravitational framework [15], a photo-absorption process between the photon and the electron in the intergalactic medium, see Equation (3) in [4], or a plasma effect, see Equation (50) in [3], all give

$$v = c [\exp(H_0 d) - 1] \quad . \quad (5)$$

We can isolate the distance d_l in Eq. (1), obtaining the linear relation

$$d_l = \frac{cz}{H_0} \quad . \quad (6)$$

In standard cosmology, one cannot use the previous approximation when inserting d into Eq. (10) for redshifts larger than ≈ 0.1 . The previous equation needs to be generalised in standard cosmology when $z > 0.1$ with the use of both the ‘Hubble function’, see Eq. (58), and the luminosity distance, see Eq. (62).

The expression for the distance, d , in the nonlinear Eq. (5) gives the relation

$$d = \frac{\ln(z+1)c}{H_0} \quad . \quad (7)$$

A Taylor expansion around $z = 0$ of this equation gives

$$d = \frac{cz}{H_0} - \frac{1}{2} \frac{cz^2}{H_0} + \frac{1}{3} \frac{cz^3}{H_0} \quad . \quad (8)$$

In the limit $z \rightarrow 0$, the linear distance, d_l , and the nonlinear, d , are equal. The laboratory results of the line shift in dense and hot plasmas can be found in [16–20]. As a first example, the experimental verification of the redshift of the spectral line of mercury as due to the surrounding electrons can be found in Figure 1, see also [21]. A second example is given by the Balmer series $H\alpha$ line emitted by laser-produced hydrogen. A linear fit of the data in Table 1 in [23] gives the relation for the redshift of the $H\alpha$ line

$$z = 0.0042 + 0.00039N_e \quad \text{when} \quad 0.0042 < z < 0.0568 \quad , \quad (9)$$

where N_e is the electron number density. This linear relation can be visualized in Figure 2. The previous relation shows a laboratory redshift as a function of a growing density. In astrophysical plasma, we are interested in the redshift as a function of the distance when the temperature of the medium is 3K, as known from the cosmic microwave background (CMB), and its mean density is extremely low. Therefore the previous laboratory experiment is illustrative rather than quantitative.

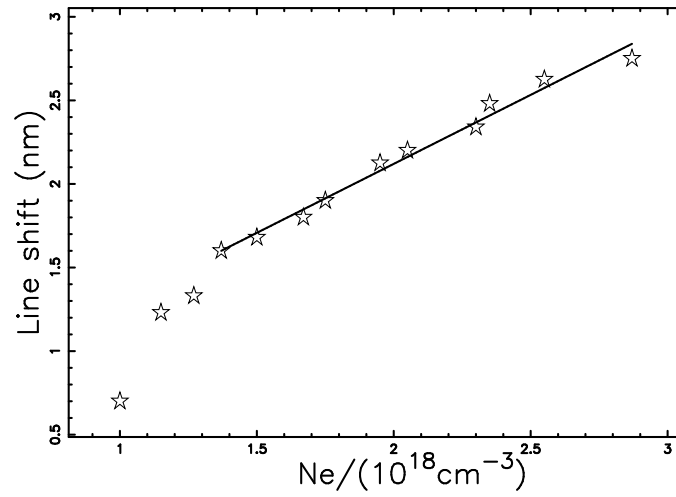


Figure 1. HgI 435.83 nm line shifts versus the electron density, data as extracted by the author from Figure 7 in [22] (empty stars) and linear regime (full line).

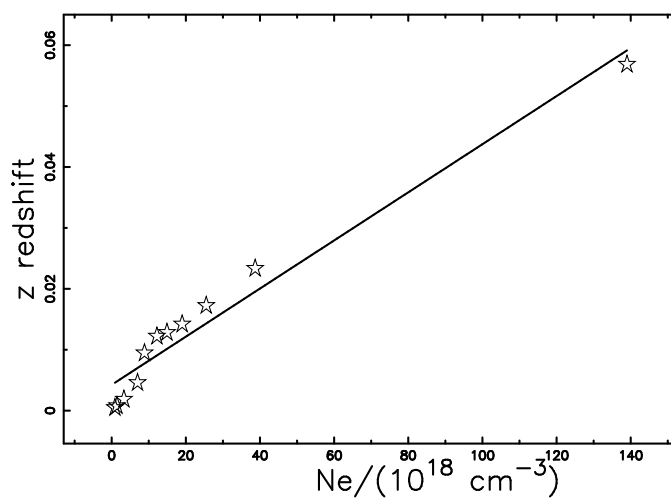


Figure 2. Redshift of the $H\alpha$ line versus the electron density, data as extracted by the author from Table 1 in [23] (empty stars) and linear fit (full line).

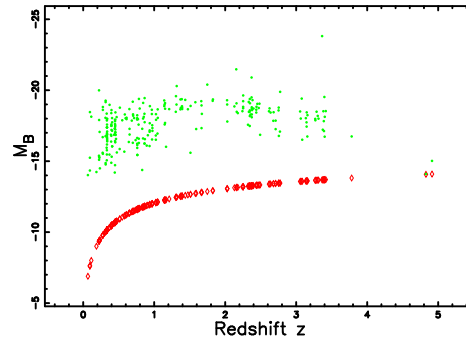


Figure 3. The blue absolute magnitude M_B computed with the nonlinear Eq. (11) for 263 galaxies belonging to the FDF catalog versus the well measured redshift. The lower theoretical curve as represented by the nonlinear Eq. (11) is the red thick line when $m_L=30.33$, which is the maximum apparent magnitude of the catalog, $\mathcal{M}_\odot = 5.48$ and $H_0 = 69.6 \text{ km s}^{-1} \text{ Mpc}^{-1}$ (green points). The redshift covers the range $[0, 4.5]$

2.1. Magnitude system

The absolute magnitude of a galaxy, M , is connected with the apparent magnitude m through the relation

$$M = m - 5 \log_{10}(d) - 25 \quad . \quad (10)$$

The nonlinear absolute magnitude as a function of the redshift as given by the nonlinear Eq. (7) is

$$M = m - 5 \log_{10} \left(\frac{\ln(z+1)c}{H_0} \right) - 25 \quad . \quad (11)$$

The previous formula predicts, from a theoretical point of view, an upper limit on the maximum absolute magnitude which can be observed in a catalog of galaxies characterized by a given limiting magnitude. The previous curve can be connected with the Malmquist bias, see [24,25], which was originally applied to the stars and later on to the galaxies by [26]. We now define the Malmquist bias as the systematic distortion in luminosity or absolute magnitude for the effective range of galaxies due to a failure in detecting those galaxies with fainter luminosity or high absolute magnitude at large distances.

Figure 3 shows such a curve, the Malmquist bias, for the FDF catalog. The well measured spectroscopic redshift, the blue and red apparent magnitude of the FDF data, can be found at the Strasbourg Astronomical Data Centre (CDS). Figure 4 shows the curve of the Malmquist bias for the zCOSMOS catalog. A careful examination of Figures 3 and 4 allows to conclude that all the galaxies are in the region over the border line of the Malmquist bias and the number of observed galaxies decreases with increasing z as theoretically predicted.

In a Euclidean, non-relativistic, and homogeneous universe, the flux of radiation without attenuation, f , expressed in units of $\frac{L_\odot}{Mpc^2}$, where L_\odot represents the luminosity of the sun, is

$$f = \frac{L}{4\pi d^2} \quad , \quad (12)$$

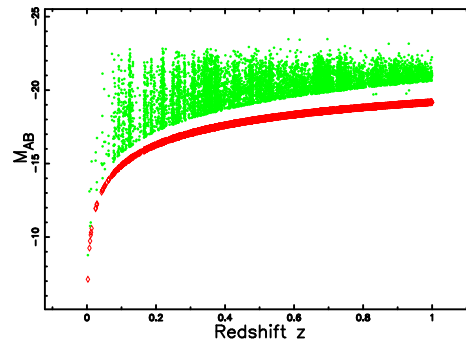


Figure 4. The B absolute magnitude M computed with the nonlinear Eq. (11) for 9697 galaxies belonging to the zCOSMOS catalog versus the redshift. The lower theoretical curve as represented by the nonlinear Eq. (11) is the red thick line when $m_L=23.2$, $M_\odot = 4.08$ and $H_0 = 69.6 \text{ km s}^{-1} \text{ Mpc}^{-1}$ (green points). The redshift covers the range $[0, 1]$

where d represents the nonlinear distance of the galaxy expressed in Mpc, see Eq. (7). The relation connecting the absolute magnitude, M , of a galaxy to its luminosity is

$$\frac{L}{L_\odot} = 10^{0.4(M_\odot - M)} \quad , \quad (13)$$

where M_\odot is the reference magnitude of the sun in the considered bandpass.

The flux expressed in units of $\frac{L_\odot}{\text{Mpc}^2}$ as a function of the apparent magnitude is

$$f = 7.957 \times 10^8 e^{0.921 M_\odot - 0.921 m} \frac{L_\odot}{\text{Mpc}^2} \quad , \quad (14)$$

and the inverse relation is

$$m = M_\odot - 1.0857 \ln(0.1256 \times 10^{-8} f) \quad . \quad (15)$$

Once a band is fixed, we have a reference magnitude of the sun in that band. We give a few examples: band u^* in SDSS $M_\odot=6.38$, band B in FDF $M_\odot=5.48$ and band B in zCOSMOS $M_\odot=4.08$.

2.2. Tired light

Assume that the photon loses energy, E , in a way proportional to its energy:

$$\frac{dE}{dt} = -Cost E \quad . \quad (16)$$

The coefficient $Cost$ is assumed to be proportional to the averaged number density of the IGM, n ,

$$Cost = an \quad , \quad (17)$$

and therefore

$$\frac{dE}{dt} = -anE \quad . \quad (18)$$

We now replace the energy $E = h\nu$ where h is Planck's constant,

$$\frac{d\nu}{dt} = -an\nu \quad , \quad (19)$$

and we convert the frequency to the wavelength,

$$\frac{d\lambda}{\lambda} = -a n dt \quad . \quad (20)$$

The speed of light, c , is assumed to be constant, $\frac{ds}{dt} = c$

$$\ln \frac{\lambda}{\lambda_0} = \frac{a}{c} \int_0^d n ds \quad , \quad (21)$$

where λ_0 is the original wavelength. On introducing the redshift

$$z = \frac{\lambda - \lambda_0}{\lambda_0} \quad , \quad (22)$$

we obtain

$$\ln(1 + z) = \frac{a}{c} < n > d \quad , \quad (23)$$

where $< n >$ is the averaged number density. The Hubble constant can be introduced with the following meaning,

$$H_0 = a < n > \quad , \quad (24)$$

obtaining

$$\ln(1 + z) = \frac{H_0}{c} d \quad . \quad (25)$$

The distance d has the same dependence on the photo-absorption/plasma process as given by Eq. (7)

$$d = \frac{\ln(z + 1) c}{H_0} \quad . \quad (26)$$

The observed flux without the absorption of our galaxy is

$$f = \frac{L}{4\pi d^2} \exp\left(-\frac{H_0}{c} d\right) = \frac{L}{4\pi d^2} \frac{1}{(1 + z)} \quad , \quad (27)$$

and the distance modulus for tired light is

$$m - M = 25 + 5 \frac{1}{\ln(10)} \ln\left(\frac{\ln(1 + z) c}{H_0}\right) + \frac{5}{2} \frac{\ln(1 + z)}{\ln(10)} \quad . \quad (28)$$

A generalization of the concept of tired light can be obtained by inserting a supplementary absorption of the light, i.e., Compton scattering, see formula (51) in [3]:

$$f = \frac{L}{4\pi d^2} \exp\left(-\frac{H_0}{c} d - 2\frac{H_0}{c} d\right) = \frac{L}{4\pi d^2} \frac{1}{(1 + z)^\beta} \quad , \quad (29)$$

where β is a variable parameter which is 1 when only tired light is considered and 3 when the Compton scattering is added. Here we have invoked the Compton scattering as a possible source of absorption but

the parameter β can be considered a regulating parameter of an unknown scattering mechanism. The distance modulus of generalized tired light without galactic extinction is

$$m - M = 25 + 5 \frac{1}{\ln(10)} \ln \left(\frac{\ln(1+z)c}{H_0} \right) + \frac{5}{2} \frac{\beta \ln(1+z)}{\ln(10)} . \quad (30)$$

Hubble's constant can be extracted from this equation as a function of the distance modulus ($m - M$):

$$H_0 = 100000 \ln(z+1) c e^{\frac{1}{2} \beta \ln(z+1) - \frac{1}{5} (m-M) \ln(10)} \text{ km s}^{-1} \text{ Mpc}^{-1} , \quad (31)$$

and, as a practical example, when $m - M = 43.834$ and $z = 0.974$, which is the case with SN C-001 in the Union 2.1 compilation, we have $H_0 = 69.6 \text{ km s}^{-1} \text{ Mpc}^{-1}$ when $\beta = 2.032$, which is the same value quoted in our Introduction.

A first comparison can be done with the distance modulus in a plasma environment as given by Eq. (7) in [27] without galactic extinction:

$$m - M = 5 \frac{\ln(\ln(z+1))}{\ln(10)} + \frac{15}{2} \frac{\ln(z+1)}{\ln(10)} + 5 \frac{1}{\ln(10)} \ln \left(\frac{c}{H_0} \right) + 25 , \quad (32)$$

see equation (7) in [27]. A second comparison can be done with the historical equation (23) in [28], which is the $[m, z]$ relation for the steady-model

$$m - M = 5 \frac{\ln(z)}{\ln(10)} + 5 \frac{\ln(1+z)}{\ln(10)} + 5 \frac{1}{\ln(10)} \ln \left(\frac{c}{H_0} \right) + 25 . \quad (33)$$

We briefly recall that Sandage [28] used two explosive models, a Friedman model [8,9] and a steady state model [29].

Figure 5 presents the behavior of the three distance moduli here considered as functions of the redshift. We now outline how formula (26) dates back to the year 1929. The original formula for the change of frequency of light in a gravitational framework is due to [15]:

$$\frac{\Delta\nu}{\nu} = \frac{1.4\pi G\rho DL}{c^2} . \quad (34)$$

Here, ν is the frequency, G is the Newtonian gravitational constant, ρ is the density in g/cm^3 , D is the distance after which the perturbing effect begins to fade out, L is the distance, and c is the speed of light.

We make the change of variables $\frac{1.4\pi G\rho DL}{c} = a < n >$, $L = ds$, $\Delta\nu = -dE/h$, and $\nu = E/h$, which means

$$\frac{dE}{E} = -\frac{a}{c} < n > ds . \quad (35)$$

On repeating the previous procedure, we obtain formula (26).

There is actually a debate on the existence of tired light in laboratory experiments. Here we use tired light as a simple theory to model a more complex interaction between light and the intergalactic plasma.

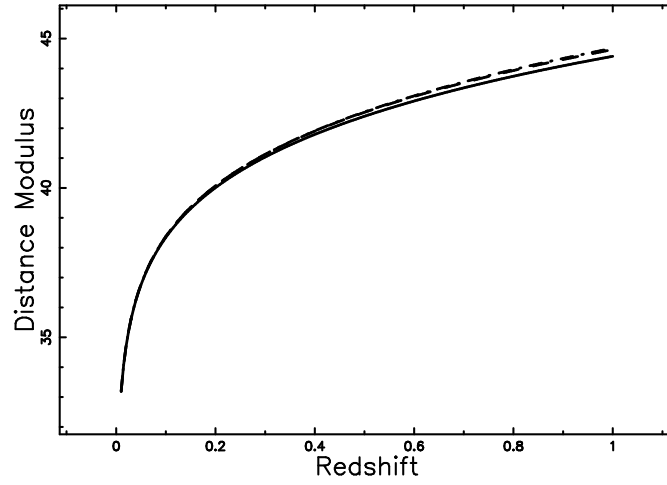


Figure 5. Distance modulus for the generalized tired light as given by Eq. (30) (full line) with $\beta=2.7$, for a plasma as given by Eq. (32) (dashed line), and for the steady-model as given by Eq. (33) (dot-dash-dot-dash line).

2.3. The luminosity function

The Schechter function, introduced by Schechter [30], provides a useful fit for the luminosity function (LF) for galaxies:

$$\Phi\left(\frac{L}{L^*}\right)dL = \left(\frac{\Phi^*}{L^*}\right)\left(\frac{L}{L^*}\right)^\alpha \exp\left(-\frac{L}{L^*}\right)dL. \quad (36)$$

Here, α sets the slope for low values of L , L^* is the characteristic luminosity, and Φ^* is a normalization. The equivalent distribution in absolute magnitude is

$$\Phi(M)dM = 0.921\Phi^*10^{0.4(\alpha+1)(M^*-M)} \exp\left(-10^{0.4(M^*-M)}\right)dM, \quad (37)$$

where M^* is the characteristic magnitude as derived from the data. The scaling with h is $M^* - 5 \log_{10} h$ and $\Phi^* h^3 [Mpc^{-3}]$.

3. N - z relation

This section evaluates the number of galaxies as a function of the redshift, firstly assuming a linear relation and secondly a nonlinear relation between redshift and distance. The evaluations are done on a sphere of radius r which is identified with the chosen distance. The main statistical test is the χ^2 :

$$\chi^2 = \sum_{i=1}^n \left(\frac{T_i - O_i}{\sigma_i} \right)^2, \quad (38)$$

where n is the number of bins, T_i is the theoretical value, O_i is the experimental value represented in terms of frequencies, and σ_i is the error computed as the square root of O_i .

3.1. The linear case

The joint distribution in z and f for galaxies, see formula (5.133) in [31] or formula (1.104) in [32] or formula (1.117) in [33], is

$$\frac{dN_l}{d\Omega dz df} = 4\pi \left(\frac{c}{H_0}\right)^5 z^4 \Phi\left(\frac{z^2}{z_{crit}^2}\right) \quad , \quad (39)$$

where $d\Omega$, dz and df represent the differential of the solid angle, the redshift, and the flux, respectively, and Φ is the Schechter LF. The critical value of z , z_{crit} , is

$$z_{l,crit}^2 = \frac{H_0^2 L^*}{4\pi f c^2} \quad . \quad (40)$$

The number of galaxies in z and f as given by formula (39) has a maximum at $z = z_{l,pos-max}$, where

$$z_{l,pos-max} = z_{crit} \sqrt{\alpha + 2} \quad , \quad (41)$$

which can be re-expressed as

$$z_{l,pos-max}(f) = \frac{\sqrt{2 + \alpha} \sqrt{10^{0.4 M_{\odot} - 0.4 M^*}} H_0}{2 \sqrt{\pi} \sqrt{f} c} \quad , \quad (42)$$

or introducing the two observable variables, M_{sun} and M^* ,

$$z_{l,pos-max}(m) = \frac{1.772 \times 10^{-5} \sqrt{2 + \alpha} \sqrt{10^{0.4 M_{\odot} - 0.4 M^*}} H_0}{\sqrt{\pi} \sqrt{e^{0.921 M_{\odot} - 0.921 m}} c} \quad . \quad (43)$$

These two formulas, which model the photometric maximum, are not reported in chapter 5 of [31].

The theoretical mean redshift of galaxies with flux f , see formula (1.105) in [32], is

$$\langle z \rangle = z_{l,crit} \frac{\Gamma(3 + \alpha)}{\Gamma(5/2 + \alpha)} \quad . \quad (44)$$

3.2. The nonlinear case

We assume that $f = \frac{L}{4\pi r^2}$ and

$$z = e^{(H_0 r/c)} - 1 \quad , \quad (45)$$

where r is the distance; in our case, d is as represented by the nonlinear Eq. (7). The relation between dr and dz is

$$dr = \frac{cdz}{(z + 1) H_0} \quad . \quad (46)$$

The joint distribution in z and f for the number of galaxies is

$$\frac{dN}{d\Omega dz df} = \frac{1}{4\pi} \int_0^\infty 4\pi r^2 dr \Phi\left(\frac{L}{L^*}\right) \delta\left(z - (e^{(H_0 r/c)} - 1)\right) \delta\left(f - \frac{L}{4\pi r^2}\right) \quad , \quad (47)$$

where δ is the Dirac delta function.

The evaluations of the integral over luminosity and distances gives

$$\frac{dN}{d\Omega dz df} = F(z; f, \Omega) = \frac{4 (\ln(z + 1))^4 c^5 \Phi^* \left(\frac{(\ln(z+1))^2}{z_{crit}^2} \right)^\alpha e^{-\frac{(\ln(z+1))^2}{z_{crit}^2}} \pi}{H_0^5 L^* (z + 1)} \quad . \quad (48)$$

The number of galaxies in z and f as given by formula 48) has a maximum at $z = z_{pos-max}$, where

$$z_{pos-max}(f) = e^{-1/16} \frac{\left(L_{star} H_0 - \sqrt{64 \pi \alpha c^2 f + 128 \pi c^2 f + L^* H_0^2 \sqrt{L^*}} \right) H_0}{\pi c^2 f} - 1 \quad , \quad (49)$$

or introducing the two observable variables, M_{sun} and M^*

$$z_{pos-max}(m) = e^{-1/16} \frac{\left(10^{0.4 M_{sun} - 0.4 M^*} H_0 - \sqrt{64 \pi \alpha c^2 f + 128 \pi c^2 f + 10^{0.4 M_{sun} - 0.4 M^*} H_0^2 \sqrt{10^{0.4 M_{sun} - 0.4 M^*}}} \right) H_0}{\pi c^2 f} - 1 \quad . \quad (50)$$

The total number of galaxies comprised between a minimum value of flux, f_{min} , and a maximum value of flux f_{max} , for the Schechter LF can be computed through the integral

$$\frac{dN}{d\Omega dz} = \int_{f_{min}}^{f_{max}} F(z; f, \Omega) df \quad . \quad (51)$$

This integral does not have an analytical expression and we must perform a numerical integration.

The theoretical mean redshift of galaxies with flux f can be deduced from Eq. (48):

$$\langle z \rangle = \frac{\int_0^\infty z F(z; f, \Omega) dz}{\int_0^\infty F(z; f, \Omega) dz} \quad . \quad (52)$$

The above integral does not have an analytical expression, and should be numerically evaluated. The differences between the formulas of this subsection and the formulas in chapter 5 of [31] are that our formalism is built to cover high values of the redshift, against the low values of the redshift of the standard approach. Both models are built in the framework of a Euclidean universe.

4. Astrophysical applications

We processed two catalogs in order to test the theoretical formulae: the FDF and the zCOSMOS. These two catalogs differ for the number of galaxies and parameters of the Schechter luminosity function (LF) for galaxies. We now review the three parameters of the Schechter LF: α is fixed, Φ^* is not relevant because we equalize the theoretical maximum in frequencies, and M^* is allowed to vary in order to match the observed frequencies. The observed mean redshift of galaxies with a flux f or m , $\langle z_{obs} \rangle$, is evaluated by the following algorithm.

1. A window in apparent magnitude or flux is chosen around m or f .
2. All the galaxies which fall in the window are selected.
3. The mean value in redshift of N selected galaxies is $\langle z_{obs} \rangle$ and the uncertainty in the mean, σ_μ , is $\sigma_\mu = s/\sqrt{N}$ where s is the standard deviation, see formula (4.14) in [34].

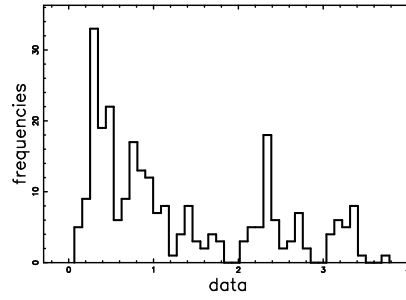


Figure 6. The galaxies of the FDF catalog are organized in frequencies versus spectroscopic redshift. The redshift covers the range $[0, 4]$ and the histogram's interval is 0.1.

4.1. The FDF catalog

The pencil beam catalog FDF has a solid angle of ≈ 5.6 sq arcmin, or $7' \times 7'$ around the south galactic pole, and covers the interval $[0, 4]$ in redshift. In particular, we selected the 263 galaxies with spectroscopical redshift and we processed the B band which has the range in apparent magnitude $[19.5, 30.2]$ mag. The reference magnitude for FDF in the B band is $\mathcal{M}_{\odot} = 5.48$. The Schechter LF for galaxies has been widely used to parametrise the LF in FDF as a function of the redshift. As an example in band B, $\alpha = -1.07$ in the range $0.45 \leq z \leq 1.11$ with $-19.52 \leq M^* \leq -18.80$, see Figure 5 in [12]. We have maintained $\alpha = -1.07$ but we make M^* variable and specify it in the captions of the figures. The distribution of the spectroscopic redshifts in the FDF is presented in Figure 6 and a comparison should be made with the distribution of photometric redshifts, see Figure 2 in [13].

Figure 7 presents the number of observed galaxies in the FDF catalog at a random apparent magnitude and Figure 8 reports the theoretical number of galaxies as function of redshift and apparent magnitude. Here we adopted the law of the rare events or Poisson distribution in which the variance is equal to the mean, i.e. the error bar is given by the square root of the frequency. An enlarged discussion on the validity of this approximation can be found in [35].

A careful examination of Figure 3 in [13] gives the maximum frequency of galaxies with well measured spectroscopic redshift in the FDF at $z \approx 0.3$. The mean redshift of galaxies as a function of the apparent magnitude for the FDF catalog is presented in Figure 9, which shows an acceptable agreement between the data (empty stars) and the theoretical values (full line).

4.2. The zCOSMOS catalog

The zCOSMOS bright redshift 10k catalog, which covers a solid angle $\Omega = 1.7 \text{ deg}^2$ or $\Omega = 3.04617 \cdot 10^{-4} \text{ sr}$, consists of 9697 galaxies in the the interval $[0, 4]$ in redshift and range in the I_B band $[15, 23]$ mag, see [14]. The reference magnitude for zCOSMOS in the I_B band is $\mathcal{M}_{\odot} = 4.08$, see Table 2.1 in [36]. The number of galaxies as a function of the redshift does not have a continuous behavior: rather, we are in the presence of an alternating behavior of voids and relative maxima, see Figure 10. This nonhomogeneous spatial distribution of galaxies can be made continuous by introducing bigger

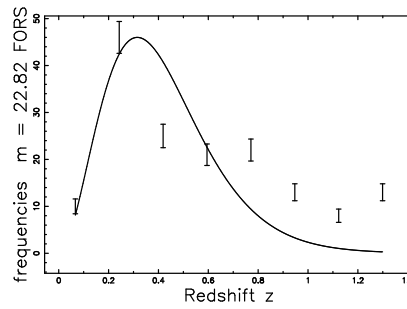


Figure 7. The galaxies of the FDF catalog with $22.08 \leq m \leq 26.81$ or $2.33 \frac{L_{\odot}}{Mpc^2} \leq f \leq 181.39 \frac{L_{\odot}}{Mpc^2}$ are organized in frequencies versus spectroscopic redshift. The redshift covers the range $[0, 1.5]$ and the histogram's interval is 0.18. The maximum frequency of observed galaxies is at $z = 0.33$, $\chi^2 = 77.8$, and the number of bins is 8. The full line is the theoretical curve generated by $\frac{dN}{d\Omega dz df}(z)$ as given by the application of the Schechter LF which is Eq. (48) with $\Phi^* = 0.01 / Mpc^3$, $M^* = -17.78$ and $\alpha = -1.07$.

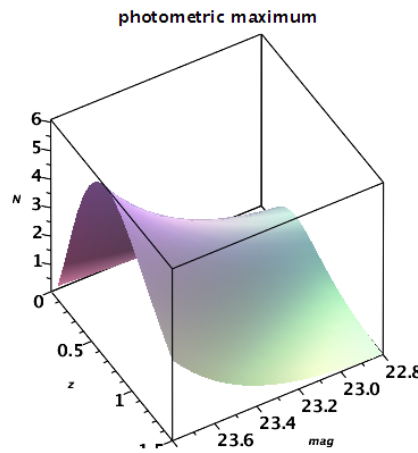


Figure 8. The theoretical number of galaxies of the FDF catalog as a function of redshift and apparent magnitude represented as a 3D surface, parameters as in Figure 7.

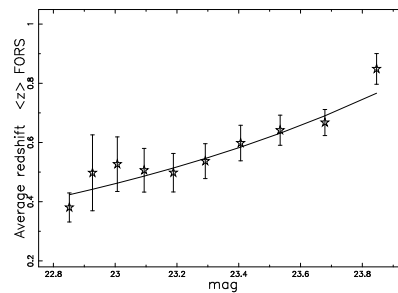


Figure 9. Average observed redshift, $\langle z_{obs} \rangle$, as a function of the apparent magnitude for the FDF catalog (empty stars) and theoretical full line for $\langle z \rangle$ as given by the numerical integration of Eq. (52). Theoretical parameters as in Figure 7.

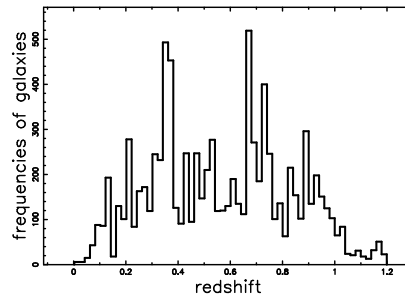


Figure 10. The galaxies of the zCOSMOS catalog are organized in frequencies versus spectroscopic redshift. The redshift covers the range $[0, 1.2]$ and the histogram's interval is 0.02.

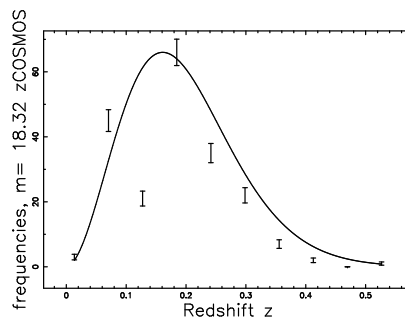


Figure 11. The galaxies of the zCOSMOS catalog with $17.88 \leq m \leq 19.06$ or $803.43 \frac{L_{\odot}}{Mpc^2} \leq f \leq 2392.36 \frac{L_{\odot}}{Mpc^2}$ are organized in frequencies versus spectroscopic redshift. The redshift covers the range $[0, 1]$ and the interval in the histogram is 0.1. The error bar is given by the square root of the frequency (Poisson distribution). The maximum frequency of observed galaxies is at $z = 0.213$, $\chi^2 = 147.3$, and the number of bins is 10. The full line is the theoretical curve generated by $\frac{dN}{d\Omega dz df}(z)$ as given by the application of the Schechter LF, which is Eq. (48) with $\Phi^* = 0.01 / Mpc^3$, $M^* = -20.88$ and $\alpha = -1.07$.

intervals in the computation of the frequencies, e.g., a histogram interval equal to 0.1. Figure 11 presents the number of observed galaxies in the zCOSMOS catalog for a given apparent magnitude.

The total number of galaxies, $\frac{dN}{d\Omega dz}$, can be computed with the integral represented by Eq. (51), see Figure 12.

The mean redshift of galaxies as a function of the apparent magnitude for zCOSMOS is presented in Figure 13.

5. The relativistic case

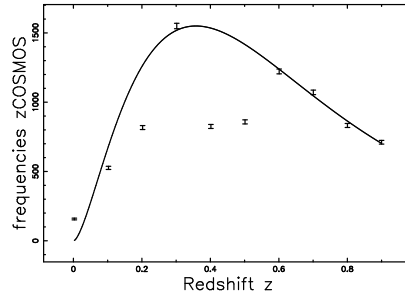


Figure 12. All the galaxies of the zCOSMOS catalog, organized in frequencies versus spectroscopic redshift. The redshift covers the range $[0, 1]$ and the interval in the histogram is 0.1. The error bar is given by the square root of the frequency (Poisson distribution). The maximum frequency of all observed galaxies is at $z = 0.35$, $\chi^2 = 1864.65$, and the number of bins is 10. The full line is the theoretical curve generated by $\frac{dN}{d\Omega dz}(z)$ as given by the numerical integration of Eq. (51) with $\Phi^* = 0.01 / Mpc^3$, $M^* = -18$ and $\alpha = -1.07$.

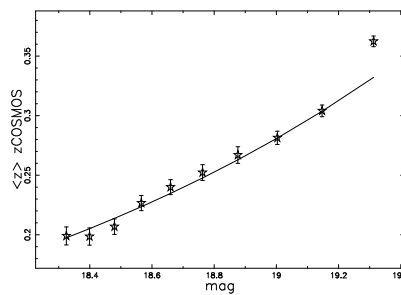


Figure 13. Average observed redshift, $\langle z_{obs} \rangle$, as a function of the apparent magnitude for the zCOSMOS catalog (empty stars) and theoretical full line, $\langle z \rangle$, as given by the numerical integration of Eq. (52). Theoretical parameters as in Figure 11.

The possibility of deriving an analytical result for the number of galaxies as a function of the redshift in the relativistic case is connected with the availability of an analytical expression for the luminosity distance. We now use the same symbols as in [37] and we define the *Hubble distance* D_H as

$$D_H \equiv \frac{c}{H_0} \quad . \quad (53)$$

We then introduce a first parameter Ω_M

$$\Omega_M = \frac{8\pi G \rho_0}{3 H_0^2} \quad , \quad (54)$$

where G is the Newtonian gravitational constant and ρ_0 is the mass density at the present time. A second parameter is Ω_Λ

$$\Omega_\Lambda \equiv \frac{\Lambda c^2}{3 H_0^2} \quad , \quad (55)$$

where Λ is the cosmological constant, see [31]. The two previous parameters are connected with the curvature Ω_K by

$$\Omega_M + \Omega_\Lambda + \Omega_K = 1 \quad . \quad (56)$$

The comoving distance, D_C , is

$$D_C = D_H \int_0^z \frac{dz'}{E(z')} \quad (57)$$

where $E(z)$ is the ‘Hubble function’

$$E(z) = \sqrt{\Omega_M (1+z)^3 + \Omega_K (1+z)^2 + \Omega_\Lambda} \quad . \quad (58)$$

The transverse comoving distance D_M is

$$D_M = \begin{cases} D_H \frac{1}{\sqrt{\Omega_K}} \sinh [\sqrt{\Omega_K} D_C / D_H] & \text{for } \Omega_K > 0 \\ D_C & \text{for } \Omega_K = 0 \\ D_H \frac{1}{\sqrt{|\Omega_K|}} \sin [\sqrt{|\Omega_K|} D_C / D_H] & \text{for } \Omega_K < 0 \end{cases} \quad (59)$$

An analytic expression for D_M can be obtained when $\Omega_\Lambda = 0$:

$$D_M = D_H \frac{2 [2 - \Omega_M (1 - z) - (2 - \Omega_M) \sqrt{1 + \Omega_M z}]}{\Omega_M^2 (1 + z)} \quad \text{for } \Omega_\Lambda = 0. \quad (60)$$

A new form for D_M when $\Omega_\Lambda = 0$ is

$$D_M = \frac{D_H \sinh \left(2 \operatorname{arctanh} \left(\frac{1}{\sqrt{1 - \Omega_M}} \right) - 2 \operatorname{arctanh} \left(\frac{\sqrt{z \Omega_M + 1}}{\sqrt{1 - \Omega_M}} \right) \right)}{\sqrt{1 - \Omega_M}} \quad . \quad (61)$$

The luminosity distance is

$$D_L = (1 + z) D_M \quad (62)$$

which in the case of $\Omega_\Lambda = 0$ becomes

$$D_L = (1 + z) \frac{D_H \sinh \left(2 \operatorname{arctanh} \left(\frac{1}{\sqrt{1 - \Omega_M}} \right) - 2 \operatorname{arctanh} \left(\frac{\sqrt{z \Omega_M + 1}}{\sqrt{1 - \Omega_M}} \right) \right)}{\sqrt{1 - \Omega_M}} \quad , \quad (63)$$

and the distance modulus

$$m - M = 25 + 5 \frac{1}{\ln(10)} \ln \left(2 \frac{c(2 - \Omega_M(1 - z) - (2 - \Omega_M)\sqrt{z\Omega_M + 1})}{H_0\Omega_M^2} \right) . \quad (64)$$

We now return to $D_L = r$: the ration between the differential of the luminosity distance and the differential of the redshift is

$$dr = \frac{c\Omega_M (2\sqrt{\Omega_M z + 1} + \Omega_M - 2) dz}{H_0\sqrt{\Omega_M z + 1}\Omega_M^2} . \quad (65)$$

This means that we have an analytical expression for the differential $dr = f(z)dz$ when $\Omega_\Lambda = 0$. This analytical differential will be inserted later on in eqn.(67). The inverse relation between distance and redshift, now denoted by z_M , is

$$z_M = \frac{rH_0\Omega_M^2 + c\Omega_M^2 - \sqrt{c\Omega_M^2(2rH_0 + c)}\Omega_M - 2c\Omega_M + 2\sqrt{c\Omega_M^2(2rH_0 + c)}}{2c\Omega_M} . \quad (66)$$

The joint distribution in z and f for the number of galaxies in the relativistic case is

$$\frac{dN}{d\Omega dz df} = \frac{1}{4\pi} \int_0^\infty 4\pi r^2 dr \Phi\left(\frac{L}{L^*}\right) \delta(z - z_M) \delta\left(f - \frac{L}{4\pi r^2}\right) , \quad (67)$$

and its explicit value is

$$\frac{dN}{d\Omega dz df} = \frac{DNN}{DND} , \quad (68)$$

where

$$DNN = 64 \Phi \left(\sqrt{\Omega_M + 1}\Omega_M + \Omega_M - 2\sqrt{\Omega_M + 1} - \Omega_M + 2 \right)^4 \times \quad (69)$$

$$\left(4 \frac{(\sqrt{\Omega_M + 1}\Omega_M + \Omega_M - 2\sqrt{\Omega_M + 1} - \Omega_M + 2)^2}{\Omega_M^4 z_{crit}^2} \right)^\alpha \times \quad (70)$$

$$e^{-4 \frac{(\sqrt{\Omega_M + 1}\Omega_M + \Omega_M - 2\sqrt{\Omega_M + 1} - \Omega_M + 2)^2}{\Omega_M^4 z_{crit}^2}} \left(2\sqrt{\Omega_M + 1} + \Omega_M - 2 \right) c^5 \pi , \quad (71)$$

and

$$DND = \Omega_M^9 \sqrt{\Omega_M z + 1} H_0^5 L^* . \quad (72)$$

Figure 14 presents the number of observed galaxies in the zCOSMOS catalog for a given apparent magnitude in the relativistic case; we adopted the value of $\Omega_M = 0.286$ because it is the concordance value, see [7].

The mean numerical redshift of galaxies as a function of the apparent magnitude for zCOSMOS is presented in Figure 15 for the relativistic case.

The observed galaxy number over-density on cosmological scales up to second order in perturbation theory with all relativistic effects that arise by observing on the past lightcone are discussed in [38,39].

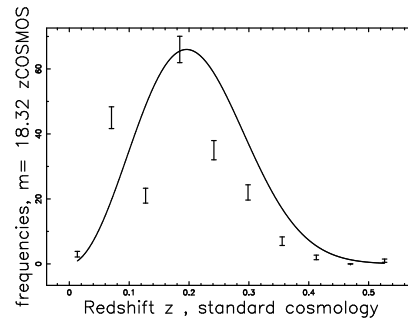


Figure 14. The galaxies of the zCOSMOS catalog with the same parameters of Figure 11 are organized in frequencies versus spectroscopic redshift. The full line is the theoretical curve generated by $\frac{dN}{d\Omega dz df}(z)$ as given by the application of the Schechter LF in the relativistic case, which is Eq. (68) with $\Phi^* = 0.01 / Mpc^3$, $M^* = -20.7$, $\alpha = -1.07$ and $\Omega_M = 0.286$; $\chi^2 = 95.68$ when the number of bin is 10.

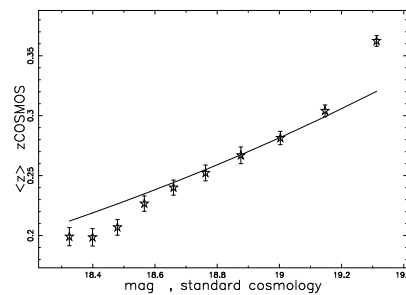


Figure 15. Average observed redshift, $\langle z_{obs} \rangle$, as function of the apparent magnitude for the zCOSMOS catalog (empty stars) and theoretical full line, $\langle z \rangle$, as given by a numerical integration. Theoretical parameters as in Figure 14.

6. Evolutionary effects

The main problem in modelling the LF as a function of the redshift is that the low luminosity galaxies progressively disappear. This observational fact can be solved by adopting a truncated probability density function (PDF). The beta distribution is defined in $[0, 1]$ and the beta with scale PDF is defined in $[0, b]$. On introducing a truncation in the beta PDF at low values, we can model the observed LF as a function of the redshift, see formula (34) in [40]. Once the random variable X is substituted with the luminosity L , we obtain a new LF for galaxies, Ψ ,

$$\Psi(L)dL = K_L \Psi^* L^{\alpha-1} (L_b - L)^{\beta-1} dL, \quad (73)$$

where Ψ^* is a normalization factor which defines the overall density of galaxies, a number per cubic Mpc. The constant K_L is

$$\begin{aligned} K_L &= \frac{A}{B} \\ A &= -\alpha \Gamma(\alpha + \beta) \\ B &= L_b^{\beta-1} {}_2F_1(\alpha, -\beta + 1; 1 + \alpha; \frac{L_a}{L_b}) L_a^\alpha \Gamma(\alpha + \beta) \\ &\quad - L_b^{\beta+\alpha-1} \Gamma(1 + \alpha) \Gamma(\beta), \end{aligned} \quad (74)$$

and L_a, L_b are the lower, upper values in luminosity and ${}_2F_1(a, b; c; z)$ is the regularized hypergeometric function [41,42]. The averaged luminosity, $\langle L \rangle$, is

$$\langle L \rangle = K_L \Psi^* \frac{A_N}{B_D}, \quad (75)$$

where

$$\begin{aligned} A_N &= -L_b^{\beta-1} L_a^{1+\alpha} {}_2F_1(-\beta + 1, 1 + \alpha; 2 + \alpha; \frac{L_a}{L_b}) \Gamma(1 + \alpha + \beta) \\ &\quad + L_b^{\alpha+\beta} \Gamma(2 + \alpha) \Gamma(\beta) \\ B_D &= (1 + \alpha) \Gamma(1 + \alpha + \beta). \end{aligned}$$

The relations connecting the absolute magnitude M , M_a and M_b of a galaxy to the respective luminosities are

$$\frac{L}{L_\odot} = 10^{0.4(M_\odot - M)}, \frac{L_a}{L_\odot} = 10^{0.4(M_\odot - M_a)}, \frac{L_b}{L_\odot} = 10^{0.4(M_\odot - M_b)}, \quad (76)$$

where M_\odot is the absolute magnitude of the sun in the considered band. The beta truncated LF in magnitude is

$$\begin{aligned} \Psi(M)dM &= -K_M \Psi^* 0.4 \left(10^{-0.4 am + 0.4 M_\odot} \right)^{\alpha-1} \times \\ &\quad \left(10^{-0.4 M_b + 0.4 M_\odot} - 10^{-0.4 am + 0.4 M_\odot} \right)^{\beta-1} \times \\ &\quad 10^{-0.4 am + 0.4 M_\odot} \ln(10) dM, \end{aligned} \quad (77)$$

where

$$\begin{aligned}
 K_M &= \frac{A_M}{B_M} \\
 A_M &= \alpha \Gamma(\alpha + \beta) \\
 B_M &= - \left(10^{-0.4M_b+0.4M_\odot} \right)^{\beta-1} \times \\
 &\quad {}_2F_1(\alpha, -\beta + 1; 1 + \alpha; \frac{10^{-0.4M_a+0.4M_\odot}}{10^{-0.4M_b+0.4M_\odot}}) \times \\
 &\quad \left(10^{-0.4M_a+0.4M_\odot} \right)^\alpha \Gamma(\alpha + \beta) \\
 &\quad + \left(10^{-0.4M_b+0.4M_\odot} \right)^{\beta+\alpha-1} \Gamma(1 + \alpha) \Gamma(\beta) .
 \end{aligned} \tag{78}$$

This LF contains the five parameters α , β , M_a , M_b , Ψ^* which can be derived from the operation of fitting the observational data and M_\odot which characterize the considered band, see [43]. The number of variables can be reduced to three once M_a and M_b are identified with the maximum and the minimum absolute magnitude of the considered sample. A further reduction of parameters can be realized in the case of a well defined catalog of galaxies, e.g., zCOSMOS, where $M_a = -23.47$ mag, $\alpha = 0.01$, $\beta = 5$ and $M_\odot = 4.08$. The low luminosity bound (high magnitude) can be modelled in the *classic case* by extracting the absolute magnitude from Eq. (28) which represents the distance modulus for tired light by

$$M_b = m_L - \frac{5}{2} \frac{\ln(1+z)}{\ln(10)} - 25 - 5 \frac{1}{\ln(10)} \ln \left(\frac{\ln(1+z)c}{H_0} \right) , \tag{79}$$

where m_L is the limiting apparent magnitude, which for zCOSMOS is $m_L = 23.2$ mag. With the above choice of parameters, the observed LF for zCOSMOS as a function of the redshift has only one free parameter, Ψ^* , which can be easily derived from the fit of the histograms. The observed LF for zCOSMOS can be built by adopting the following algorithm.

1. A value for the redshift is fixed, z , as well as the thickness of the layer, Δz .
2. All the galaxies comprised between z and Δz are selected.
3. The absolute magnitude can be computed from Eq. (28) which represents the distance modulus for tired light.
4. The distribution in magnitude is organized in frequencies versus absolute magnitude.
5. The frequencies are divided by the volume, which is $V = \Omega \pi r^2 \Delta r$, where r is the considered radius, Δr is the thickness of the radius, and Ω is the solid angle of ZCOSMOS.
6. The error in the observed LF is obtained as the square root of the frequencies divided by the volume.

Figures 16, 17, and 18 present the LF of zCOOSMOS as well the fit with the truncated beta LF at $z = 0.2$, $z = 0.5$, and $z = 0.7$, respectively.

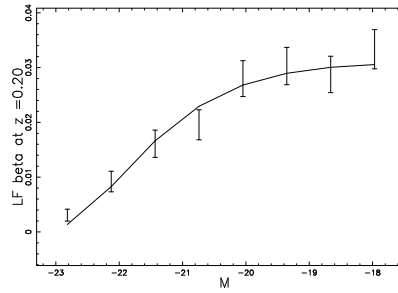


Figure 16. The luminosity function data of zCOSMOS are represented with error bars. The continuous line fit represents our beta LF (77), the parameters are $z = 0.2$, $\Delta z=0.05$ and $\text{NDIV} = 8$, which means $\chi^2 = 5.35$.

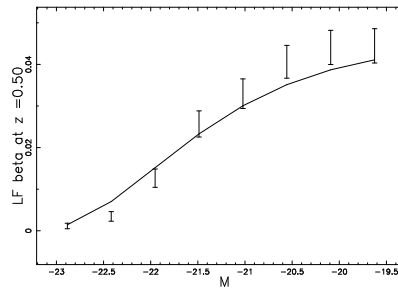


Figure 17. The luminosity function data of zCOSMOS are represented with error bars. The continuous line fit represents our beta LF (77), the parameters are $z = 0.5$, $\Delta z=0.05$, and $\text{NDIV} = 8$, which means $\chi^2 = 16.71$.

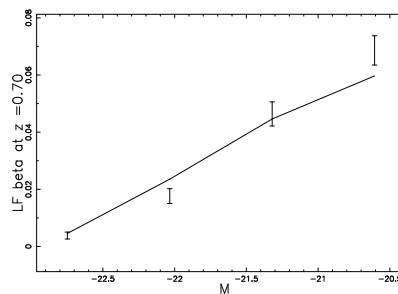


Figure 18. The luminosity function data of zCOSMOS are represented with error bars. The continuous line fit represents our beta LF (77), the parameters are $z = 0.7$, $\Delta z=0.03$, and $\text{NDIV} = 4$, which means $\chi^2 = 8.76$.

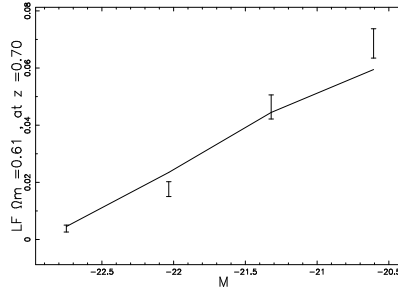


Figure 19. The luminosity function data of zCOSMOS are represented with error bars. The continuous line fit represents our beta LF (77) in the relativistic case. The input parameters are $\Omega_\Lambda = 0$, $\Omega_M = 0.286$, $z = 0.7$, $\Delta z = 0.03$ and $\text{NDIV} = 4$, which means $\chi^2 = 8.78$.

In the relativistic case, we can extract the absolute magnitude from Eq. (64), which represents the distance modulus when $\Omega_\Lambda = 0$:

$$M_b = m_l - 5 \frac{\ln(2)}{\ln(10)} - 5 \frac{1}{\ln(10)} \ln \left(\frac{c(2 - \Omega_M(1 - z) - (2 - \Omega_M)\sqrt{z\Omega_M + 1})}{H_0 \Omega_M^2} \right) - 25 \quad (80)$$

Figure 19 presents the LF of zCOSMOS as well as the fit with the truncated beta LF when $z = 0.7$ in the relativistic case.

7. Conclusions

Results:

A nonlinear formulation of Hubble's law allows determining an old/new relation for the distance as a function of the redshift, see Equation (7). This distance, when inserted in the definition of the joint distribution in z and f for the number of galaxies, allows the determination of a new $N - z$ relation, see Eq. (48). Two photometric tests were done for 263 galaxies belonging to the FDF catalog and for 9697 galaxies belonging to the zCOSMOS catalog. The first test is dedicated to the photometric maximum in redshift, for which is possible to derive an analytical expression as a function of the flux, see Eq. (49), or the apparent magnitude, see Eq. (49); this results in Figures 7 and 11.

A second test is dedicated to the average redshift, for which a numerical integration of Eq. (52) should be done; it results in Figures 9 and 13.

The same formalism can also be applied to the relativistic case once the relativistic luminosity distance is given, see Eq. (63). In the standard cosmology or relativistic case the joint distribution in z and f for the number of galaxies is given by Eq. (68). A comparison between the Euclidean and relativistic model can be made on the photometric maximum as represented by Figures 11 and 14. The χ^2 test gives $\chi^2 = 147.3$ for the Euclidean case, as represented by Eq. (47) and $\chi^2 = 94.27$ for the relativistic case as represented by Eq. (68), but large oscillations are present in the observed frequencies and therefore the definitive answer is remanded to future efforts.

The observed LF for galaxies can be modelled by a truncated beta LF, see Eq. (77). This new LF with an appropriate choice of parameters has only one free parameter, which is the number of galaxies per

cubic Mpc, Ψ^* , and this parameter decreases with the redshift. The high magnitude bound, M_b , can be modelled both by a Euclidean model as given by Eq. (79) and by a relativistic model, $\Omega_\Lambda = 0$, as given by Eq. (80). As an example, the third test for the observed LF for galaxies at $z = 0.7$ gives $\chi^2 = 8.76$ for the Euclidean case and $\chi^2 = 8.78$ for the relativistic case when $\Omega_\Lambda = 0$ and $\Omega_M = 0.286$.

Generalized tired light:

The presence of the factor β for adjustable tired light, see Eqs. (29) and (30), poses the problem of its determination. Eq. (30), which represents the distance modulus, can be calibrated on the database of supernova (SN) of type Ia. A careful determination of β and H_0 can provide a better determination of the Malmquist bias, as represented by Figures 3 and 4, which present a lack of galaxies just above the red lines.

Tired light versus GR

The new distance modulus as represented by Eq. (30) requires a careful comparison with the standard LCDM. In the case of LCDM with $\Omega_\Lambda = 0$, an analytical solution for the luminosity distance exists and allows the determination of the relation between the differential of the distance and the differential of the redshift, see Eq. (65).

In the case of $\Omega_\Lambda \neq 0$, an analytical expression for the luminosity distance does not exist, and as a consequence we do not have at the moment of writing a relation between the differential of the distance and the differential of the redshift. The use of the Padé approximant can produce analytical results for the luminosity distance, see [44,45]; this approximation will be the subject of future research.

The cells

The cellular structure of our universe, see as an example Figure 10, is now the greatest inconvenience to the application of the continuous models for the number of galaxies as a function of the redshift, and perhaps an explanation for why the theoretical lines do not fit the data, as an example see Figure 12. We briefly recall that there is an actual debate on the dimension of the universe which is modelled by $N \propto R^D$, where N is the number of galaxies, R the radius of the considered sphere, and D the dimension. An homogeneous universe means $D = 3$. In the concordance model, D makes a transition to $D=3$ at scales between 40 and 100 Mpc, see [46]. An accurate analysis of 2MASS Photometric Redshift catalogue (2MPZ), shows an agreement with the standard cosmological model; the homogeneous regime is reached faster than a class of fractal models with $D < 2.75$, see [47]. As an example of non-homogeneity the value $D = 1.87$ has been reported in [48] where the 2MASS Redshift Survey catalog was analysed.

Acknowledgments

I am grateful to the anonymous referee for useful suggestions which have changed the structure of the paper.

References

1. Mohr, P.J.; Taylor, B.N.; Newell, D.B. CODATA recommended values of the fundamental physical constants: 2010. *Reviews of Modern Physics* **2012**, *84*, 1527–1605.
2. Kaiser, N. Astronomical redshifts and the expansion of space. *MNRAS* **2014**, *438*, 2456–2465, [arXiv:astro-ph.CO/1312.1190].

3. Brynjolfsson, A. Redshift of photons penetrating a hot plasma. *arXiv:astro-ph/0401420* **2004**.
4. Ashmore, L. Recoil Between Photons and Electrons Leading to the Hubble Constant and CMB. *Galilean Electrodynamics* **2006**, *17*, 53.
5. Crawford, D.F. Observational Evidence Favors a Static Universe (Part I). *Journal of Cosmology* **2011**, *13*, 3875–3946.
6. Marmet, L. Survey of Redshift Relationships for the Proposed Mechanisms at the 2nd Crisis in Cosmology Conference. Astronomical Society of the Pacific Conference Series; F. Potter., Ed., 2009, Vol. 413, *Astronomical Society of the Pacific Conference Series*, pp. 315–335.
7. Bennett, C.L.; Larson, D.; Weiland, J.L.; Hinshaw, G. The 1% Concordance Hubble Constant. *ApJ* **2014**, *794*, 135, [[1406.1718](#)].
8. Friedmann, A. Über die Krümmung des Raumes. *Zeitschrift für Physik* **1922**, *10*, 377–386.
9. Friedmann, A. Über die Möglichkeit einer Welt mit konstanter negativer Krümmung des Raumes. *Zeitschrift für Physik* **1924**, *21*, 326–332.
10. Riess, A.G.; Filippenko, A.V.; Challis, P.; Clocchiatti, A. Observational Evidence from Supernovae for an Accelerating Universe and a Cosmological Constant. *AJ* **1998**, *116*, 1009–1038, [[astro-ph/9805201](#)].
11. Perlmutter, S.; Aldering, G.; Goldhaber, G.; Knop, R.A. Measurements of Omega and Lambda from 42 High-Redshift Supernovae. *ApJ* **1999**, *517*, 565–586, [[astro-ph/9812133](#)].
12. Gabasch, A.; Bender, R.; Seitz, S.; Hopp, U.; Saglia, R.P.; Feulner, G.; Snigula, J.; Drory, N.; Appenzeller, I.; Heidt, J.; Mehlert, D.; Noll, S.; Böhm, A.; Jäger, K.; Ziegler, B.; Fricke, K.J. The evolution of the luminosity functions in the FORS Deep Field from low to high redshift. I. The blue bands. *A&A* **2004**, *421*, 41–58, [[astro-ph/0403535](#)].
13. Appenzeller, I.; Bender, R.; Böhm, A.; Frank, S.; Fricke, K.; Gabasch, A.; Heidt, J.; Hopp, U.; Jäger, K.; Mehlert, D.; Noll, S.; Saglia, R.; Seitz, S.; Tapken, C.; Ziegler, B. Exploring Cosmic Evolution with the FORS Deep Field. *The Messenger* **2004**, *116*, 18–24.
14. Lilly, S.J.; Le Brun, V.; Maier, C.; Mainieri, V. The zCOSMOS 10k-Bright Spectroscopic Sample. *ApJS* **2009**, *184*, 218–229.
15. Zwicky, F. On the Red Shift of Spectral Lines through Interstellar Space. *Proceedings of the National Academy of Science* **1929**, *15*, 773–779.
16. Nguyen, H.; Koenig, M.; Benredjem, D.; Caby, M.; Coulaud, G. Atomic structure and polarization line shift in dense and hot plasmas. *Phys. Rev. A* **1986**, *33*, 1279–1290.
17. Leng, Y.; Goldhar, J.; Griem, H.R.; Lee, R.W. C vi Lyman line profiles from 10-ps KrF-laser-produced plasmas. *Phys. Rev. E* **1995**, *52*, 4328–4337.
18. Saemann, A.; Eidmann, K.; Golovkin, I.E. Isochoric heating of solid aluminum by ultrashort laser pulses focused on a tamped target. *Physical Review Letters* **1999**, *82*, 4843–4846.
19. Zhidkov, A.G.; Sasaki, A.; Tajima, T. Direct spectroscopic observation of multiple-charged-ion acceleration by an intense femtosecond-pulse laser. *Physical Review E* **1999**, *60*, 3273–3278.
20. Wang, H.; Yang, X.; Li, X. Ground-State Energy Shifts of H-Like Ti Under Dense and Hot Plasma Conditions. *Plasma Science and Technology* **2007**, *9*, 128–132.
21. Ashmore, L. Intrinsic Plasma Redshifts Now Reproduced In The Laboratory - a Discussion in Terms of New Tired Light. *viXra:Astrophysics:1105.0010* **2011**.

22. Chen, C.S.; Zhou, X.L.; Man, B.Y.; Zhang, Y.Q.; Guo, J. Investigation of the mechanism of spectral emission and redshifts of atomic line in laser-induced plasmas. *Optik* **2009**, *120*, 473–478.
23. Kielkopf, J.F.; Allard, N.F. Shift and width of the Balmer series H α line at high electron density in a laser-produced plasma. *Journal of Physics B Atomic Molecular Physics* **2014**, *47*, 155701.
24. Malmquist, K. A study of the stars of spectral type A. *Lund Medd. Ser. II* **1920**, *22*, 1–10.
25. Malmquist, K. On some relations in stellar statistics. *Lund Medd. Ser. I* **1922**, *100*, 1–10.
26. Behr, A. Zur Entfernungsskala der extragalaktischen Nebel. *Astronomische Nachrichten* **1951**, *279*, 97–107.
27. Brynjolfsson, A. Magnitude-Redshift Relation for SNe Ia, Time Dilation, and Plasma Redshift. *ArXiv:astro-ph/0602500* **2006**.
28. Sandage, A. The Ability of the 200-INCH Telescope to Discriminate Between Selected World Models. *ApJ* **1961**, *133*, 355.
29. Hoyle, F.; Sandage, A. The Second-Order Term in the Redshift-Magnitude Relation. *PASP* **1956**, *68*, 301.
30. Schechter, P. An analytic expression for the luminosity function for galaxies. *ApJ* **1976**, *203*, 297–306.
31. Peebles, P.J.E. *Principles of physical cosmology*; Princeton University Press: Princeton, N.J., 1993.
32. Padmanabhan, T. *Cosmology and Astrophysics through Problems*; Cambridge University Press: Cambridge, UK, 1996.
33. Padmanabhan, P. *Theoretical astrophysics. Vol. III: Galaxies and Cosmology*; Cambridge University Press: Cambridge, UK, 2002.
34. Bevington, P. R. and Robinson, D. K.. *Data Reduction and Error analysis for the physical sciences*; McGraw-Hill: New York, 2003.
35. Aggarwal, R.; Caldwell, A. Error bars for distributions of numbers of events. *The European Physical Journal Plus* **2012**, *127*, 1–8.
36. Binney, J.; Merrifield, M. *Galactic astronomy*; Princeton University Press: Princeton, NJ, 1998.
37. Hogg, D.W. Distance measures in cosmology. *ArXiv Astrophysics e-prints* **1999**, [[astro-ph/9905116](#)].
38. Bertacca, D.; Maartens, R.; Clarkson, C. Observed galaxy number counts on the lightcone up to second order: I. Main result. *Journal of Cosmology and Astroparticle Physic* **2014**, *9*, 37, [[1405.4403](#)].
39. Bertacca, D.; Maartens, R.; Clarkson, C. Observed galaxy number counts on the lightcone up to second order: II. Derivation. *Journal of Cosmology and Astroparticle Physic* **2014**, *11*, 13, [[1406.0319](#)].
40. Zaninetti, L. The initial mass function modeled by a left truncated beta distribution. *ApJ* **2013**, *765*, 128–135.
41. Abramowitz, M.; Stegun, I.A. *Handbook of Mathematical Functions with Formulas, Graphs, and Mathematical Tables*; Dover: New York, 1965.

42. Olver, F.W.J.e.; Lozier, D.W.e.; Boisvert, R.F.e.; Clark, C.W.e. *NIST handbook of mathematical functions.*; Cambridge University Press. : Cambridge, 2010.
43. Zaninetti, L. The Luminosity Function of Galaxies as Modeled by a Left Truncated Beta Distribution. *International Journal of Astronomy and Astrophysics* **2014**, *4*, 145–154, [[arXiv:astro-ph.CO/1403.2558](#)].
44. Adachi, M.; Kasai, M. An Analytical Approximation of the Luminosity Distance in Flat Cosmologies with a Cosmological Constant. *Progress of Theoretical Physics* **2012**, *127*, 145–152, [[arXiv:astro-ph.CO/1111.6396](#)].
45. Wei, H.; Yan, X.P.; Zhou, Y.N. Cosmological applications of Pade approximant. *Journal of Cosmology and Astroparticle Physic* **2014**, *1*, 45, [[arXiv:astro-ph.CO/1312.1117](#)].
46. Bagla, J.S.; Yadav, J.; Seshadri, T.R. Fractal dimensions of a weakly clustered distribution and the scale of homogeneity. *MNRAS* **2008**, *390*, 829–838, [[0712.2905](#)].
47. Alonso, D.; Salvador, A.I.; Sánchez, F.J.; Bilicki, M.; García-Bellido, J.; Sánchez, E. Homogeneity and isotropy in the Two Micron All Sky Survey Photometric Redshift catalogue. *MNRAS* **2015**, *449*, 670–684, [[1412.5151](#)].
48. Zaninetti, L. Revisiting the Cosmological Principle in a Cellular Framework. *Journal of Astrophysics and Astronomy* **2012**, *33*, 399–416, [[arXiv:astro-ph.CO/1212.6838](#)].

© 2015 by the author; licensee MDPI, Basel, Switzerland. This article is an open access article distributed under the terms and conditions of the Creative Commons Attribution license (<http://creativecommons.org/licenses/by/4.0/>).